

# Bisphosphonate-Linked TrkB Agonist: Cochlea-Targeted Delivery of a Neurotrophic Agent as a Strategy for the Treatment of Hearing Loss

Judith S. Kempfle,<sup>†,‡,§</sup> Kim Nguyen,<sup>||</sup> Christine Hamadani,<sup>†,‡</sup> Nicholas Koen,<sup>†,‡</sup> Albert S. Edge,<sup>†,‡</sup> Boris A. Kashemirov,<sup>||</sup> David H. Jung,<sup>\*,†,‡</sup> and Charles E. McKenna<sup>\*,||</sup> 

<sup>†</sup>Department of Otolaryngology and The Eaton-Peabody Laboratories, Massachusetts Eye and Ear Infirmary, Boston, Massachusetts 02114, United States

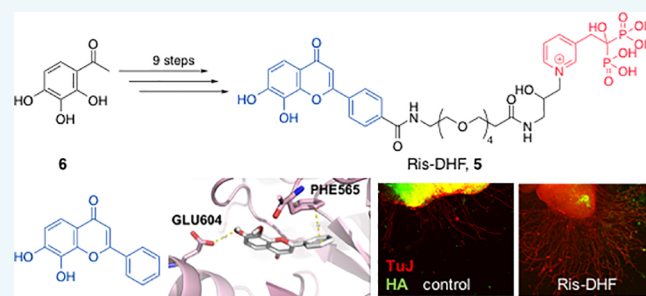
<sup>‡</sup>Department of Otolaryngology and Laryngology, Harvard Medical School, Boston, Massachusetts 02114, United States

<sup>§</sup>Department of Otolaryngology, University of Tübingen Medical Center, Tübingen 72076, Germany

<sup>||</sup>Department of Chemistry, University of Southern California, Los Angeles, California 90089-0744, United States

 Supporting Information

**ABSTRACT:** Hearing loss affects more than two-thirds of the elderly population, and more than 17% of all adults in the U.S. Sensorineural hearing loss related to noise exposure or aging is associated with loss of inner ear sensory hair cells (HCs), cochlear spiral ganglion neurons (SGNs), and ribbon synapses between HCs and SGNs, stimulating intense interest in therapies to regenerate synaptic function. 7,8-Dihydroxyflavone (DHF) is a selective and potent agonist of tropomyosin receptor kinase B (TrkB) and protects the neuron from apoptosis. Despite evidence that TrkB agonists can promote survival of SGNs, local delivery of drugs such as DHF to the inner ear remains a challenge. We previously demonstrated in an animal model that a fluorescently labeled bisphosphonate, 6-FAM-Zol, administered to the round window membrane penetrated the membrane and diffused throughout the cochlea. Given their affinity for bone mineral, including cochlear bone, bisphosphonates offer an intriguing modality for targeted delivery of neurotrophic agents to the SGNs to promote survival, neurite outgrowth, and, potentially, regeneration of synapses between HCs and SGNs. The design and synthesis of a bisphosphonate conjugate of DHF (Ris-DHF) is presented, with a preliminary evaluation of its neurotrophic activity. Ris-DHF increases neurite outgrowth *in vitro*, maintains this ability after binding to hydroxyapatite, and regenerates synapses in kainic acid-damaged cochlear organ of Corti explants dissected *in vitro* with attached SGNs. The results suggest that bisphosphonate–TrkB agonist conjugates have promise as a novel approach to targeted delivery of drugs to treat sensorineural hearing loss.



## INTRODUCTION

Age-related sensorineural hearing loss (SNHL) affects nearly two-thirds of adults 70 and older.<sup>1</sup> SNHL is associated with irreversible degeneration of the sensory cells of the auditory portion of the inner ear (cochlea), including hair cells (HCs) and spiral ganglion neurons (SGNs).<sup>2</sup> Emerging evidence has highlighted an additional, previously underappreciated etiology of hearing loss—that of primary synaptopathy, or loss of synapses between HCs and SGNs. Thus, noise exposure or aging can lead to loss of ribbon synapses between SGNs and HCs in murine models and humans.<sup>3–6</sup> Primary synaptopathy has been termed “hidden hearing loss” as it may underlie subtle discriminatory functions of the ear, such as hearing in a noisy environment, rather than grossly changing the thresholds at which sound is detected.<sup>7</sup> After synaptic degradation, or after damage of the sensory epithelium of the cochlea with loss of neurotrophic support, SGNs retract peripheral neurites and

slowly degenerate.<sup>8</sup> Notably, the cell bodies of SGNs persist long after hair cells and synapses have disappeared, for months in mice<sup>5</sup> and possibly decades in humans.<sup>9</sup> Current treatment for SNHL relies solely on amplification of sound (hearing aids) or, in severe cases of SNHL, on electrical stimulation of remaining neurons (cochlear implants).<sup>10</sup> However, such modalities do not fully restore a biologic hearing experience.

The persistence of SGN cell bodies raises the possibility that exogenous neurotrophins might support SGN survival, induce neurite outgrowth, and even regenerate synapses with surviving hair cells to improve hearing. Neurotrophins play a critical role in SGN development and maintenance<sup>8,11</sup> and have been shown to promote SGN survival and enhance neurite

Received: January 8, 2018

Revised: February 6, 2018

outgrowth and synaptogenesis.<sup>12–15</sup> Strikingly, overexpression of a neurotrophin within the cochlea via genetic manipulation<sup>16</sup> and local application of neurotrophin protein to the cochlea<sup>17</sup> have both been shown to regenerate cochlear synapses following noise damage.

Current drug delivery methods to the inner ear include diffusion across the round window membrane (RWM), direct infusion via cochleostomy, or systemic delivery.<sup>18</sup> With respect to neurotrophin delivery, prior model systems have utilized local methods to locally deliver viral vectors carrying a neurotrophin gene or whole neurotrophin protein, such as brain derived neurotrophic protein (BDNF) or neurotrophin-3 (NT-3), after damaging or destroying hair cells or synapses.<sup>17,19–22</sup> However, cochlear viral delivery in the setting of hearing preservation has proven to be challenging, and delivery of whole proteins across the intact human RWM, as opposed to the rodent RWM, may similarly prove to be difficult.<sup>22,23</sup> Small molecule drugs, such as 7,8-dihydroxyflavone (DHF, **1**), a tropomyosin receptor kinase B (TrkB) agonist,<sup>24</sup> provide a potential alternative solution for regenerative treatment of neurons. DHF effectively promotes SGN survival, supports sprouting *in vitro*, and protects SGNs from *in vivo* degeneration in the setting of connexin-26 mutation and hair cell loss.<sup>25,26</sup> However, drug application of native DHF to the RWM may have a debilitating limitation in that the delivered compound may remain present for an insufficient amount of time before being cleared by inner ear fluids.<sup>27,28</sup>

We have therefore sought to identify a novel method to anchor neurotrophic activity in the cochlea. Bisphosphonates (BPs), such as risedronate (Ris) or zoledronate (Zol), whose chemical structures mimic pyrophosphate, are characterized by strong affinity to bone mineral and are widely used clinically to treat resorptive bone disorders such as osteoporosis.<sup>29</sup> Prior work has demonstrated that BPs can conjugate to fluorescent dyes to image bone<sup>30,31</sup> and to antibiotics for bone-targeted drug delivery.<sup>32</sup> We previously showed that 6-FAM-Zol, a fluorescein–BP conjugate,<sup>33,35</sup> readily enters the mammalian cochlea through the RWM and labels the modiolus and osseus spiral lamina, the location of SGNs.<sup>34,36</sup>

In this study, we report the design and synthesis of a novel BP conjugate with DHF (Ris-DHF, **5**) and evaluate its potential for bone-targeted neurotrophic stimulation of damaged SGNs and for reinnervation of cochlear hair cells.

## RESULTS AND DISCUSSION

**Chemistry.** *Design of a Bisphosphonate-Modified TrkB Agonist.* As the TrkB agonist, we selected **1** (Figure 1) due to its well established specificity and potency.<sup>24</sup> To determine a suitable site for linker attachment (i.e., compatible with retention of agonist activity), **1** was modeled into the crystal structure of TrkB (PDB code 4AT3)<sup>37</sup> after deletion of the cocrystallized Cpd5n (a TrkB inhibitor), using AutoDock Vina.<sup>38</sup> This study revealed several potential binding interactions of **1** in the agonist binding site, including 7-OH hydrogen bonding with GLU604 and  $\pi$ -stacking of the phenyl ring with PHE565 (Figure 1A and 1B) (cf. Cpd5n bound within the site, Figure 1C). In this preferred pose, the phenyl ring of **1** (circled in red) is facing outward from the binding pocket, suggesting permissible modification at the 3- or 4-carbon.

Subsequent docking results (data not shown) with the 4-phenyl carboxyl 7,8-DHF derivative **2** (COOH-DHF, Figure 2) encouraged us to select it as the linkable form of **1**. We initially

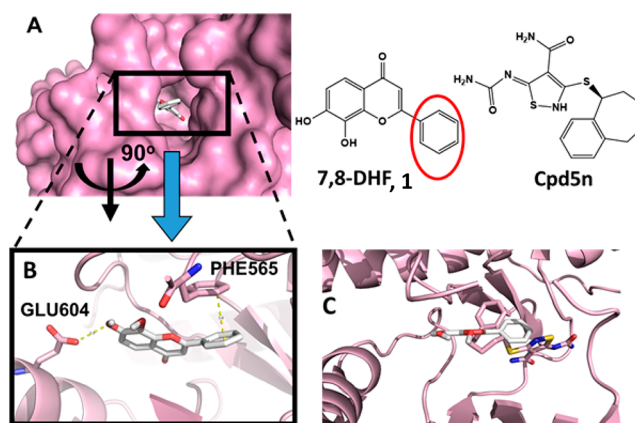


**Figure 1.** Molecular docking of **1** into the TrkB agonist site (PDB code: 4AT3) using AutoDock Vina. A. Overview of **1** docked into the binding site of TrkB. B. Zoomed view of the predicted preferred binding pose of **1**. C. Zoomed view comparing the predicted pose of **1** with the experimentally determined configuration of Cpd5n in the TrkB active site.

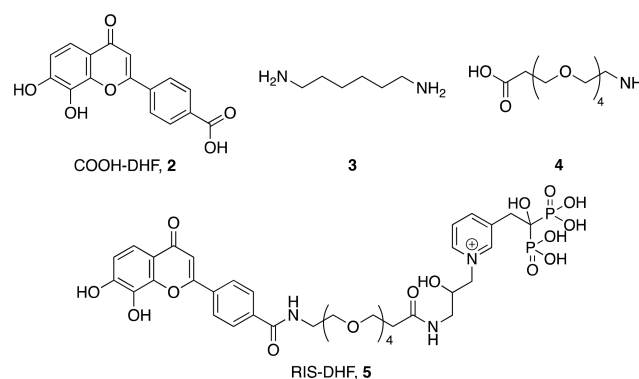
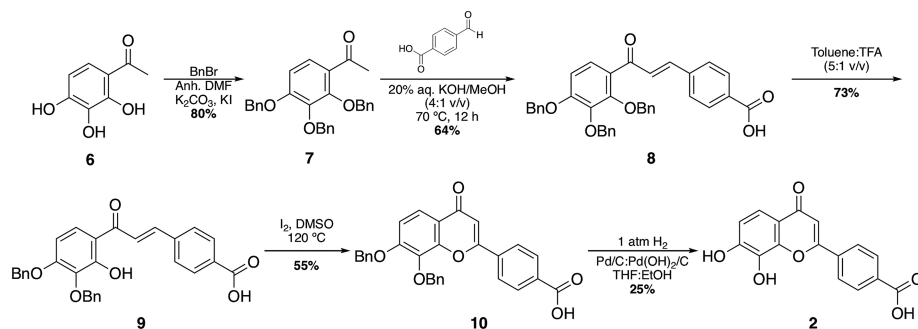


**Figure 2.** Structures of COOH-DHF, **2**, linkers **3** and **4**, and RIS-DHF, **5**.

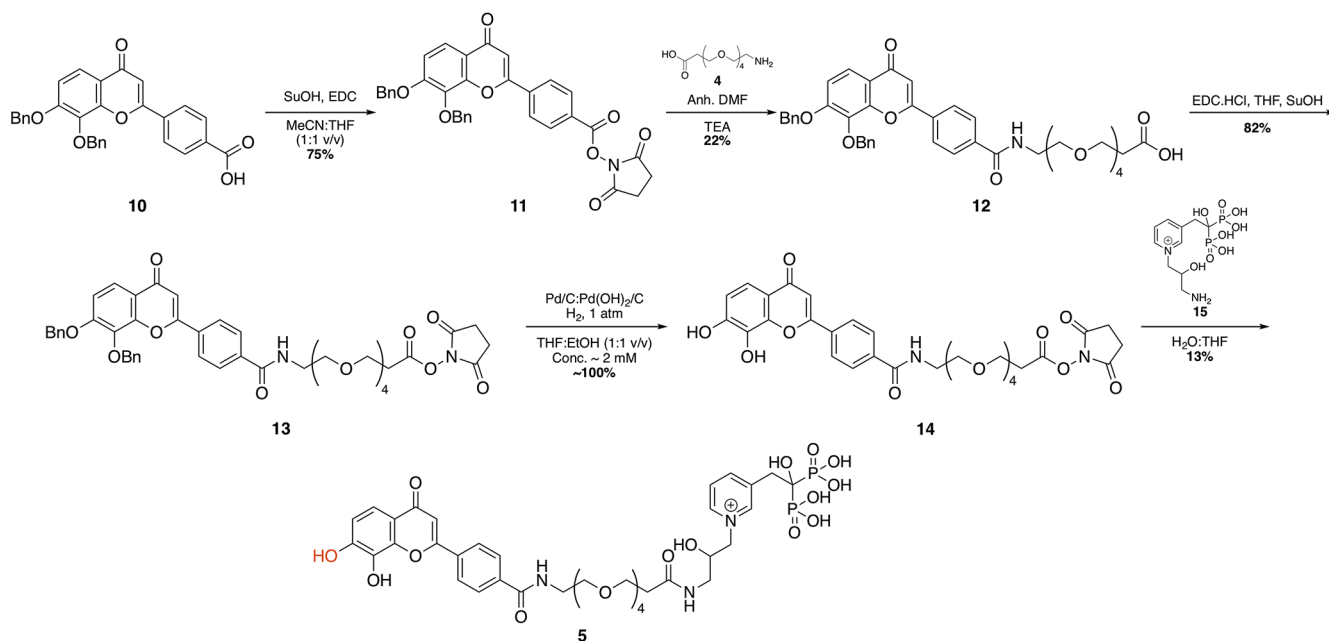
considered 1,6-diaminohexane (**3**) as the linker molecule and carried out preliminary synthetic studies using this approach (details, Supporting Information) but ultimately turned to a more polar and water-soluble PEG linker, 15-amino-4,7,10,13-tetraoxopentadecanoic acid (**4**). Based on our previous studies showing that fluorescently labeled Ris and Zol bind strongly to cochlear bone,<sup>39</sup> we chose Ris as the BP, adapted for linking by attachment of a 1-amino-2-hydroxypropane-3-diyl group at the pyridyl nitrogen, which led to the target compound, **5** (Ris-DHF, Figure 2).

**Synthesis.** The synthesis of **1** has been previously reported by Sun et al.<sup>40</sup> A similar route was followed to prepare **2**, beginning from tribenylation of 2,3,4-trihydroxybenzophenone (**6**) followed by aldol condensation of the product **7** with 4-carboxybenzaldehyde (replacing benzaldehyde in the literature synthesis of **1**) in 20% aq. KOH/EtOH at 50 °C, giving the adduct **8** which was then reacted with TFA to remove the 2-benzyl group, forming **9** (Scheme 1). This sequence of steps, in reversing the recommended order in the **1** synthesis,<sup>40</sup> improved the overall yield of **9** from <20% to ~50%. Cyclization promoted by heating with a catalytic amount (0.1 equiv) of I<sub>2</sub> in DMSO then gave the dibenzyl-protected *p*-carboxyflavone **10**, which was converted to **2** by treatment with 1 atm H<sub>2</sub> over Pd/C: Pd(OH)<sub>2</sub>/C in 1:1 THF:EtOH.

Scheme 1. Synthesis of COOH-DHF, 2



Scheme 2. Synthesis of RIS-DHF, 5



Conversion of **10** to its activated *N*-succinyl ester **11** allowed facile amidation with the PEG linker **4** in anhydrous DMF (to **12**), and *N*-succinyl esterification of the distal free linker carboxyl acid group in this intermediate (**12** to **13**) followed by removal of the two remaining benzyl groups, again by catalytic hydrogenation, provided **14** (Scheme 2). This compound was reacted with the linkable Ris derivative **15**<sup>30</sup> in H<sub>2</sub>O/THF (pH adjusted to 8.3 with Na<sub>2</sub>CO<sub>3</sub>) to give the final target compound **5** (13%).

Compound **5** was purified by gradient RP-HPLC (0.1 M triethylammonium bicarbonate buffer (pH 7.0) containing 10% and then 75% of acetonitrile). A p*K*<sub>a</sub> calculation (Marvin Sketch 15.12.14.0) indicated that the 7-OH group (red, Scheme 2) is deprotonated at pH 7 (p*K*<sub>a</sub> calculated, 6.6), thus the <sup>1</sup>H NMR sample was coevaporated with 70% MeOH, 0.1 M ammonium acetate buffer (pH 5.0) and then dissolved in D<sub>2</sub>O, which provided good peak resolution. **5** was further characterized by MS and <sup>31</sup>P NMR spectroscopy.

**Biology.** *Ris-DHF Promotes Spiral Ganglion Neurite Outgrowth in Vitro.* To study the effect of Ris-DHF on spiral ganglion neurite outgrowth, postnatal (P4) SGNs were plated in culture and subjected to treatment with 400 nM of Ris, DHF, Ris-DHF, or control with DMSO for 48 h (Figure 3). Immunohistochemical and quantitative analysis of neuron-specific class III Tubulin (TuJ1) positive neurites revealed an

average neurite outgrowth of 0.248 mm (±SEM 0.0483) for control samples. Average outgrowth for treated samples was 0.294 mm (±0.0308) for Ris, 0.445 mm (±SEM 0.0506) for DHF, and 0.421 mm (±0.0490) for Ris-DHF. The relative ratio of treated samples to control demonstrated a significant increase of fiber length after treatment with DHF and Ris-DHF compared to Ris alone or control (Figure 3A-B). DHF promoted a slightly longer average neurite outgrowth than Ris-DHF, but this difference was not statistically significant (*p* = 0.32). Neurite outgrowth with Ris alone did not significantly differ from control. To gain insight into the mechanism of action of Ris-DHF, we investigated whether Ris-DHF acts through TrkB, the receptor for BDNF and DHF. TrkB is phosphorylated upon binding to BDNF<sup>41,42</sup> or DHF,<sup>43</sup> and we identified phosphorylated TrkB along elongating neurites of SGNs treated with Ris-DHF (Figure 3C). Treatment with ANA12, a noncompetitive inhibitor of TrkB,<sup>44</sup> appeared to abrogate SGN neurite outgrowth in the presence of DHF or Ris-DHF (Figure 3D). Taken together, these results suggest that the ability of DHF to promote spiral ganglion neurite outgrowth via TrkB was preserved following conjugation to Ris in the hybrid Ris-DHF molecule.

*Ris-DHF Promotes Neurite Outgrowth after Binding to Hydroxyapatite.* To evaluate the functional ability of Ris-DHF to promote neurite outgrowth when bound to hydroxyapatite

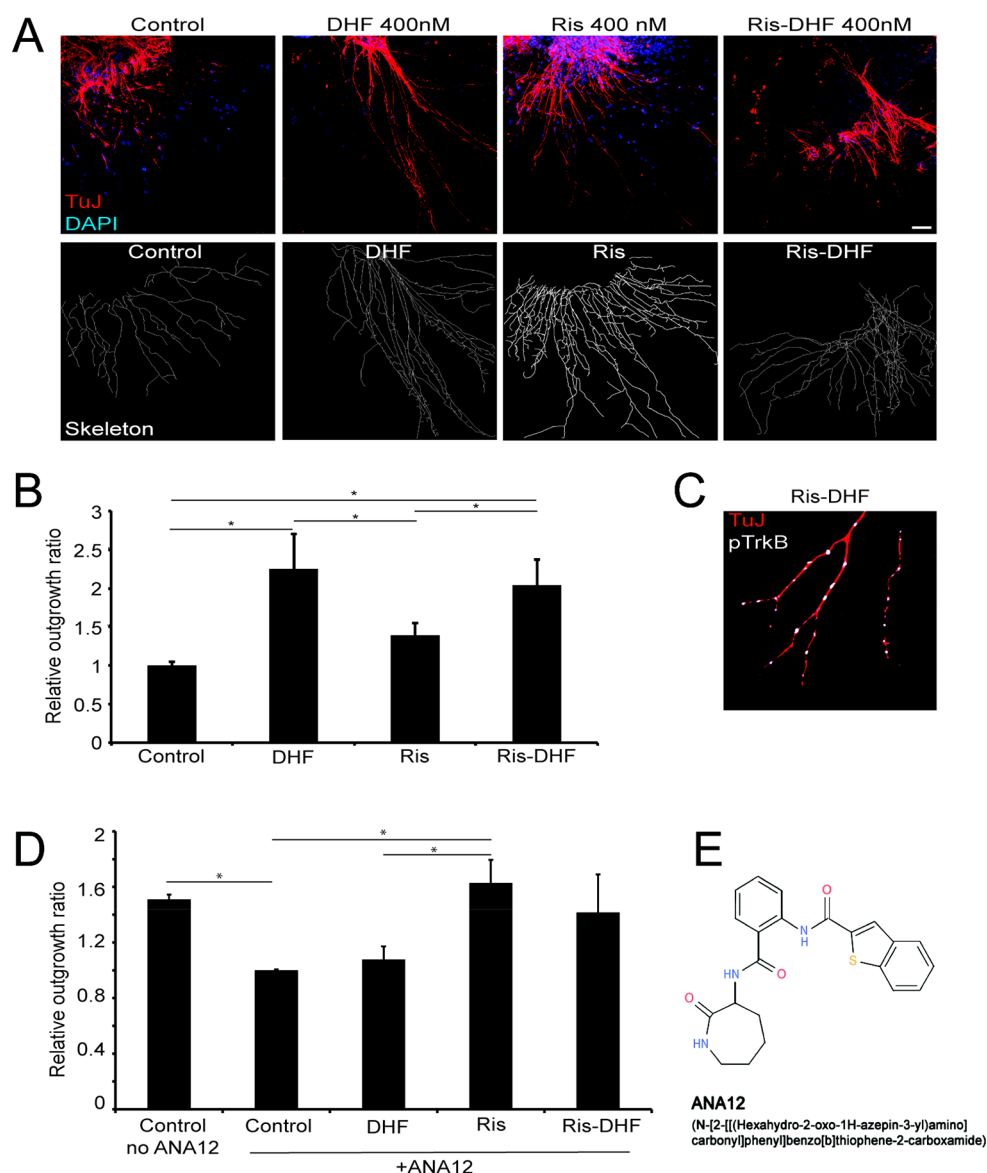


**Figure 3.** Spiral ganglion neurite outgrowth *in vitro*. **A.** Immunohistochemical analysis of cochlear SGNs after 48 h in culture, treated with 400 nM DHF, 400 nM Ris, 400 nM Ris-DHF, or DMSO as a control. Neurons were stained with neural marker TuJ1 (red); nuclei are labeled with DAPI (blue). Scale bar represents 100  $\mu\text{m}$ . Neurite outgrowth length was measured with 3D Neurite Tracer, and total traces were processed and rendered into a tagged 3D skeleton. **B.** Relative ratio of neurite lengths across experiments ( $n = 7$ ) was calculated compared to control. Results are expressed as mean  $\pm$  SEM (\* represents  $p < 0.05$ ). **C.** Phosphorylated TrkB (pTrkB) puncta visualized along elongated neurites. **D.** 10 nM ANA12, an inhibitor of TrkB, decreases DHF- and Ris-DHF-mediated neurite outgrowth. Results are expressed as relative outgrowth ratios to Control with ANA12 ( $n = 4$ ). Results are expressed as mean  $\pm$  SEM (\* represents  $p < 0.05$ ). **E.** Structure of ANA12.

(HA, the primary component of bone matrix), we preincubated HA nanoparticles for 1 h with DHF, Ris, Ris-DHF, or DMSO. For easier visualization of particles, we added a small amount of Fam-Ris, a fluorescent derivative of risedronate,<sup>30</sup> to all samples. Washed particles were then plated with SGNs for 48 h in regular growth medium to evaluate neurite outgrowth driven by HA-bound drug. Analysis and quantification revealed that HA-bound Ris-DHF promoted significantly more outgrowth as compared to HA-bound Ris or control. Ris promoted some neurite outgrowth compared to untreated control, suggesting a minor positive effect of Ris on neurites. As expected, DHF preincubation with HA did not produce a significant increase in neurite outgrowth (Figure 4A and B). Qualitatively, we observed neurite outgrowth paths in response to HA-bound Ris-DHF to be more convoluted than in response

to Ris-DHF in solution (compare Figure 3A and 4A). Higher power magnification revealed that neurites both terminated upon HA-Ris-DHF pellets and traveled past the pellets (Figure 4C). Taken together, these data demonstrate that neurite outgrowth driven by Ris-DHF is maintained after binding to HA.

**Ris-DHF Promotes Regeneration of Cochlear Ribbon Synapses *In Vitro*.** To assess the ability of Ris-DHF to stimulate synaptic regeneration, we adapted a well-established *in vitro* model for cochlear synaptopathy.<sup>45</sup> Organ of Corti (OC) explants with attached neurons were dissected and plated and then treated with kainic acid (KA) to induce excitotoxic damage to ribbon synapses.<sup>45</sup> After 2 h of treatment, synaptic damage and neurite retraction were confirmed (data not shown), and explants were treated with soluble DHF, Ris, Ris-

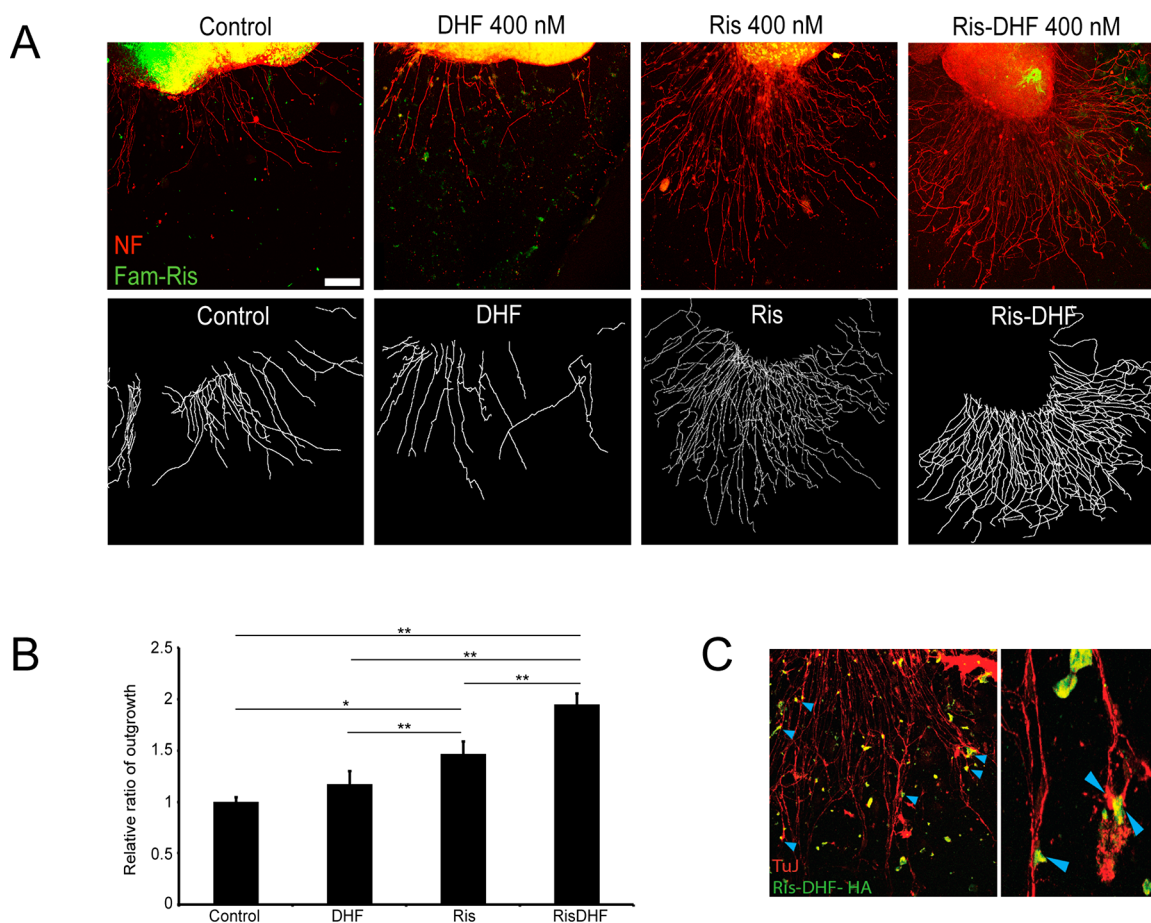


**Figure 4.** Prebinding to hydroxyapatite bone matrix does not inhibit 400 nM Ris-DHF-promoted neurite outgrowth *in vitro*. **A.**  $\sim 500 \mu\text{g}$  HA nanoparticles prebound to 400 nM of Ris, DHF, Ris-DHF, or DMSO control were plated with SGNs for 48 h. Total traces were processed and rendered into a tagged 3D skeleton (white). **B.** Neurite outgrowth length was measured via 3D Neurite Tracer software, and each neurite was individually traced through its z-stack. Relative ratio of neurite lengths across total experiments ( $n = 8$ ) was calculated. Results are expressed as mean  $\pm$  SEM (\* represents  $p < 0.05$ ; \*\* represents  $p < 0.01$ ). **C.** Neurites were observed to both grow past (single blue arrowhead) and terminate upon (double blue arrowheads) HA-Ris-DHF nanoparticles.

DHF, or DMSO as control for 24 h. After fixation, regenerated synapses were visualized using immunohistochemistry and confocal microscopy (Figure 5). The juxtaposition of pre- and postsynaptic portions of the ribbon synapse was considered to represent a fully regenerated synapse. The number of synapses was then quantified per inner hair cell (IHC) (Figure 5C). Each experiment was performed with an untreated control explant (no kainic acid, KA $-$ ), to evaluate synapse survival in culture at baseline. KA $-$  explants maintained 12.5 synapses/IHC ( $\pm 0.5671$ ) on average. Spontaneous synaptic regeneration was assessed with OC explants treated with KA alone (KA $+$ ). KA $+$  explants demonstrated very little spontaneous synaptic regeneration ( $1.57 \pm 0.4989$  synapses/IHC). Additional treatment with Ris-DHF significantly increased the number of regenerated synapses compared to KA $+$  ( $8.20 \pm 0.5828$  synapses/IHC). Unconjugated DHF regenerated at a comparable level (DHF:  $9.20 \pm 0.7865$  synapses/IHC;  $p$  value = 0.12 relative to Ris-DHF). Ris alone had a modest regenerative effect on synapses, albeit significantly lower ( $5.34 \pm 0.7629$  synapses/IHC) when compared to DHF or Ris-DHF. Taken together, these results suggest that the hybrid molecule Ris-DHF promotes synaptic regeneration after damage *in vitro*.

We have shown that a rationally designed bisphosphonate-DHF molecule retains neurotrophic properties of native DHF, both with respect to the promotion of spiral ganglion neurite

outgrowth and the regeneration of ribbon synapses within the OC *in vitro*. Furthermore, prebinding of Ris-DHF to HA, which simulates bone binding, preserves the ability of Ris-DHF to direct neurite outgrowth. These results highlight the promise of BPs as drug delivery molecules for the inner ear and outline a novel small molecule approach to the regeneration of cochlear synapses between HCs and SGNs.

The delivery of drugs to the inner ear presents unique opportunities and challenges.<sup>46</sup> Systemic administration may be relatively straightforward but has the potential for greater systemic side effects and decreased concentration within the inner ear following delivery. Local delivery to the cochlea across the RWM via intratympanic injection is common in outpatient clinical use in humans for the treatment of sudden hearing loss and Meniere's disease, although it remains unclear if the drugs administered in such treatments are uniquely able to cross the oval and round windows into the inner ear. Local delivery via cochleostomy has the potential for the highest delivery levels. However, opening the cochlea presents inherent risks to hearing that may be unacceptably high for patients with useful hearing, such as patients with synaptopathy. Our previous work demonstrated that BPs can enter the mammalian cochlea following delivery to the RWM and that such delivery could be achieved in a nontoxic manner.<sup>35</sup> As the cochlea is encased in bone, bisphosphonates may represent a novel way to achieve

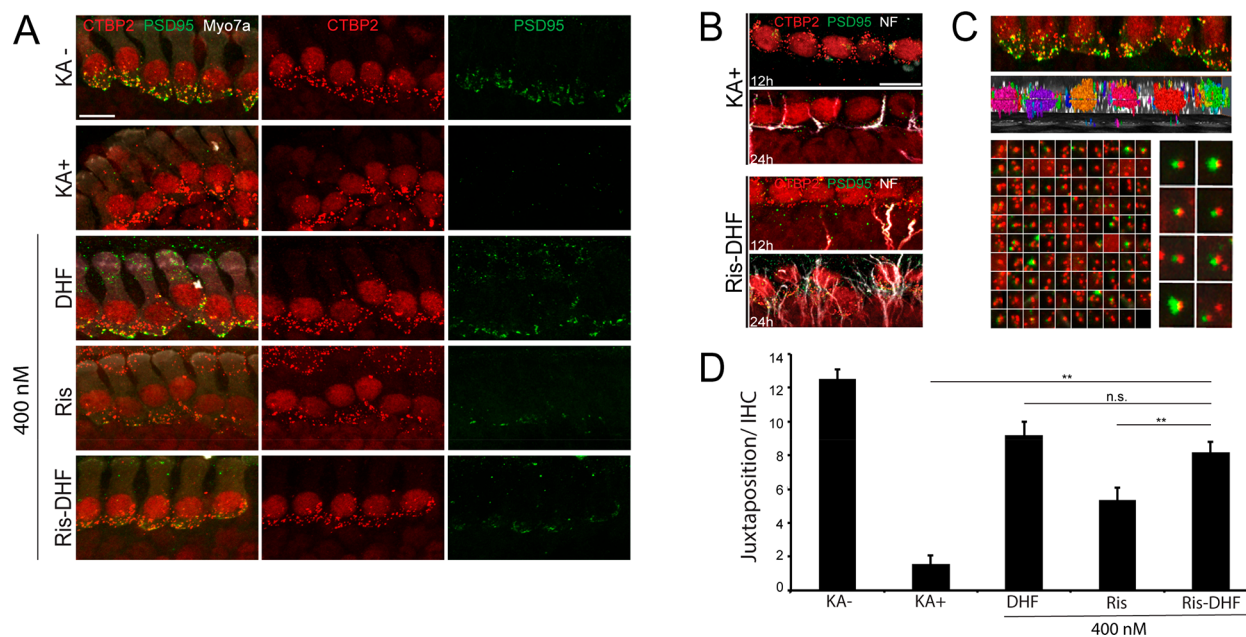


**Figure 5.** Cochlear synapse regeneration after Ris-DHF treatment in an *in vitro* synaptopathy model. **A.** Organ of Corti (OC) explants treated with 0.5 mM KA for 2 h followed by 24 h incubation with Ris 400 nM, DHF 400 nM, or Ris-DHF 400 nM. Untreated explants (KA-) or KA only treated explants (KA+) served as controls. Presynaptic synapse was stained with CtBP2 (red), which also labeled inner hair cell (IHC) cell bodies. Postsynaptic synapse (neural synapse portion) was visualized with PSD95 (green). Hair cell bodies were labeled with myosin VIIa (Myo7a, white). **B.** Regrowth of neurites following 400 nM Ris-DHF treatment at 12 h and 24 h. Neurites are visualized in white with antineurofilament antibody (NF). **C.** Computed postprocessing within 3D cubical space allowed for quantification of juxtaposed pre- and postsynaptic labels. **D.** Quantified synapses per IHC across 5 experiments compared to controls ( $n = 5$ ) at 24 h. Results are expressed as mean  $\pm$  SEM (n.s., not significant; \*\* represents  $p < 0.01$ ).

long-term cochlear drug delivery using well established clinical techniques for minimally invasive local delivery.

With respect to the inner ear, BPs appear to promote SGN survival in the setting of osteoprotegerin deficiency,<sup>47</sup> suggesting that they may have positive effects in the context of SGN survival and synaptogenesis beyond simply holding molecules of interest in place. In this regard, our results show that Ris modestly promotes neurite outgrowth following prebinding to HA. Further, Ris mediates regeneration of cochlear synapses following KA treatment, although at a lower level than either DHF or Ris-DHF. In the context of our ANA12 inhibitor data, Ris-mediated neurite outgrowth appears to act independently of TrkB, suggesting that Ris may perform this function via a parallel pathway for SGN survival or outgrowth.

Because of the critical roles of neurotrophins in development and maintenance of cochlear wiring,<sup>8,11</sup> there has been intense interest in the therapeutic use of neurotrophins to promote SGN survival and synaptic regeneration. Genetically modified mice that overexpressed a neurotrophin within the cochlea established the theoretical viability of such an approach, as these animals demonstrated an ability to regenerate cochlear synapses after noise trauma.<sup>16</sup> In this regard, the therapeutic approaches explored thus far have involved intracochlear delivery of viral particles expressing neurotrophin genes,<sup>19</sup> local topical delivery of neurotrophin proteins to the RWM,<sup>17,20</sup> and local intracochlear delivery of neurotrophin proteins in the context of a cochlear implant.<sup>21</sup> Local delivery of DHF has also been shown to promote SGN survival after massive hair cell loss.<sup>25</sup> Of these approaches, however, only topical delivery of neurotrophin proteins to the RWM has been accomplished in animals in the context of hearing preservation. The small

molecule approach we describe may therefore hold several critical advantages with respect to clinical application. First, small molecules may be more likely than proteins to cross the RWM, particularly in the setting of the more complex RWM in humans relative to rodents.<sup>23</sup> Second, we have chosen to leverage the bony anatomy of the cochlea through use of a tailored BP as an anchor for long-term stimulation of SGNs. In this regard, our previous work examining BP delivery to the cochlea has demonstrated that BPs have a high affinity for the osseous spiral lamina of the cochlea, which lies in close proximity to SGNs.<sup>35</sup> The prolonged binding of BP conjugates to bone<sup>31</sup> suggests that this approach may provide a way to overcome some of the described barriers to inner ear drug delivery, including distribution of drug among the cochlear fluids and elimination of drug from the cochlea.<sup>28</sup>

## EXPERIMENTAL PROCEDURES

**General Information.** All reagents, including 4-carboxybenzaldehyde and mono-*t*Boc-protected 1,6-diaminohexane (**18**, [Supporting Information](#)), were purchased from Sigma-Aldrich or Alfa Aesar, except as noted. Risedronate monosodium was a kind gift from Warner Chilcott (formerly P&G Pharmaceuticals). Triethylamine (TEA) was distilled from KOH, and dioxane and THF were distilled from sodium. 15-Amino-4,7,10,13-tetraoxopentadecanoic acid **4** was purchased as the *N*-Boc derivative from Chem-Impex International, Inc. Other reagents were used as supplied by the manufacturer. Flash chromatography purification was performed using a Teledyne CombiFlash Rf<sup>+</sup> Lumen system. Thin layer chromatography (TLC) was performed on Merck Silica Gel 60 F254 plates, and the developed plates were visualized under a UV lamp at 354 nm. HPLC separations were

performed on a Rainan Dynamax Model SD-200 system with a Rainan Dynamax absorbance detector Model UV-DII. NMR spectra were recorded on either Varian Mercury 400, Varian VNMR5-500, or Varian VNMR5-600 spectrometer. Chemical shifts are expressed as ppm downfield from a solvent residual ( $^1\text{H}$ ,  $^{13}\text{C}$ ) peak or an external standard ( $\text{H}_3\text{PO}_4$ ,  $^{31}\text{P}$ ). LC-MS analyses were performed on a Thermo-Finnigan LCQ DECA XP MAX Ion Trap LC/MS/MS spectrometer operated in ESI mode.

**Synthesis of the DHF Conjugate, 5.** *2,3,4-Trisbenzyloxycetophenone (7)*. In a dry 100 mL round-bottom flask, 1.7 g (10 mmol) of **6** was added to a stirred suspension of 6.0 g (35.0 mmol, 3.5 equiv) of benzyl bromide, 8.0 g (58.0 mmol) of potassium carbonate, and 0.25 g (1.5 mmol) of potassium iodide in 20 mL of anhydrous DMF. The reaction mixture was heated to 50 °C and stirred for 8 h. After cooling to rt, solid potassium carbonate was filtered, and the filtrate was diluted with 100 mL of ethyl acetate. The resulting solution was washed with water and brine and then dried over  $\text{Na}_2\text{SO}_4$ . The crude product was purified by column chromatography on silica gel using a gradient of 0–50% ethyl acetate in hexane: white solid after evaporation of solvent, 3.53 g (80%).

$^1\text{H}$  NMR (400 MHz, chloroform-*d*)  $\delta$  7.50 (d,  $J$  = 8.8 Hz, 1H), 7.47–7.19 (m, 15H), 6.81 (d,  $J$  = 8.9 Hz, 1H), 5.16 (s, 2H), 5.15 (s, 2H), 5.06 (s, 2H), 2.52 (s, 3H).

$^{13}\text{C}$  NMR (101 MHz, chloroform-*d*)  $\delta$  198.29, 156.70, 137.12, 136.17, 128.72, 128.64, 128.53, 128.51, 128.32, 128.23, 128.14, 127.52, 127.04, 125.67, 108.83, 76.37, 75.60, 70.91, 31.10.

*(E)-4-(3-Oxo-3-(2,3,4-tris(benzyloxy)phenyl)prop-1-en-1-yl)benzoic Acid (8)*. Compound **7**, 476 mg (1.09 mmol), was dissolved in 50 mL of MeOH, and 15 mL of 20% KOH was added. The suspension was heated to 70 °C and stirred until the compound was completely dissolved. 207 mg of 4-carboxybenzaldehyde (1.38 mmol, 1.3 equiv) was added. After stirring for 8 h, the mixture was cooled to rt and filtered. The pH of the filtrate was adjusted to pH 4 with acetic acid, and the filtrate was extracted with ethyl acetate. The organic layer was washed with water and brine, dried over  $\text{Na}_2\text{SO}_4$ , and evaporated, and the residue was purified by column chromatography (0–50% methanol in dichloromethane, 0.5% trifluoroacetic acid), giving 395 mg (64%) of a white solid.

$^1\text{H}$  NMR (600 MHz, chloroform-*d*)  $\delta$  9.56 (bs), 8.03 (d,  $J$  = 8.5 Hz, 2H), 7.63 (s, 2H), 7.58 (d,  $J$  = 8.8 Hz, 1H), 7.49–7.27 (m, 14H), 7.24–7.13 (m, 3H), 6.88 (d,  $J$  = 8.9 Hz, 1H), 5.19 (s, 2H), 5.12 (s, 2H), 5.09 (s, 2H).

$^{13}\text{C}$  NMR (101 MHz, chloroform-*d*)  $\delta$  189.90, 171.24, 141.73, 140.97, 136.53, 136.13, 130.55, 130.35, 129.25, 128.73, 128.68, 128.38, 128.30, 128.19, 127.55, 126.98, 126.56, 109.32, 77.00, 70.97.

*(E)-4-(3-(3,4-Bis(benzyloxy)-2-hydroxyphenyl)-3-oxoprop-1-en-1-yl)benzoic Acid (9)*. In a 100 mL round-bottom flask, 395 mg (0.69 mmol) of **8** was dissolved in 20 mL of toluene, followed by the addition of trifluoroacetic acid (TFA) (5:1 toluene:TFA v/v). After stirring for 1.5 h, the solvent was evaporated, and the product was purified by flash column chromatography (0–50% methanol in dichloromethane, 0.5% trifluoroacetic acid) giving 242 mg of a white solid (73%).

$^1\text{H}$  NMR (500 MHz, DMSO-*d*<sub>6</sub>)  $\delta$  13.18 (s, 1H), 8.22–8.08 (m, 2H), 8.06–7.95 (m, 4H), 7.87 (d,  $J$  = 15.4 Hz, 1H), 7.51–7.21 (m, 11H), 6.85 (d,  $J$  = 9.2 Hz, 1H), 5.30 (s, 2H), 5.00 (s, 2H).

$^{13}\text{C}$  NMR (101 MHz, DMSO-*d*<sub>6</sub>)  $\delta$  192.81, 167.27, 158.41, 158.11, 143.29, 139.00, 137.98, 135.43, 130.15, 129.57, 128.91, 128.62, 128.51, 128.27, 128.17, 128.04, 123.84, 115.66, 105.40, 74.38, 70.63.

*4-(7,8-Bis(benzyloxy)-4-oxo-4H-chromen-2-yl)benzoic Acid (10)*. To a solution of **9** (242 mg, 0.5 mmol) in 15 mL of DMSO was added iodine (12.7 mg, 0.1 equiv), and the mixture was heated to 120 °C. After stirring for 12 h, the reaction mixture was cooled to rt and quenched with ice cold water. A slightly yellow precipitate appeared, that was filtered. Extraction with EtOAc was performed, and the organic layer was washed with saturated  $\text{Na}_2\text{S}_2\text{O}_3$  and then brine. The solvent was removed by evaporation, and **10** was collected as a slight yellow solid residue and combined with the yellow precipitate, total yield 133.4 mg (55%).

$^1\text{H}$  NMR (400 MHz, DMSO-*d*<sub>6</sub>)  $\delta$  8.03 (s, 4H), 7.77 (d,  $J$  = 9.0 Hz, 1H), 7.54–7.50 (m, 2H), 7.47–7.29 (m, 9H), 7.01 (s, 1H), 5.35 (s, 2H), 5.19 (s, 2H).

$^{13}\text{C}$  NMR (101 MHz, DMSO-*d*<sub>6</sub>)  $\delta$  177.02, 162.30, 156.17, 150.61, 137.47, 136.77, 136.04, 129.99, 126.18, 118.53, 79.86, 79.53, 79.20, 75.69, 71.03.

*4-(7,8-Dihydroxy-4-oxo-4H-chromen-2-yl)benzoic Acid (2)*. 69 mg of **10** and a catalytic amount of 10% Pd/C (0.1 equiv) were stirred in 15 mL of a 1:1 v/v mixture of MeOH:THF. The reaction mixture was heated to 40 °C, flushed with  $\text{N}_2$  gas (3 $\times$ ), and stirred overnight under  $\text{H}_2$  at atmospheric pressure. Solids were removed by filtration, and the filtrate was evaporated at reduced pressure. The solid residue was recrystallized from methanol to give 10.6 mg of **2** (25%).

$^1\text{H}$  NMR (400 MHz, DMSO-*d*<sub>6</sub>)  $\delta$  13.25 (s, 1H), 10.34 (s, 1H), 9.51 (s, 1H), 8.26 (d,  $J$  = 8.7 Hz, 2H), 8.08 (d,  $J$  = 8.7 Hz, 2H), 7.40 (d,  $J$  = 8.7 Hz, 1H), 7.09–6.86 (m, 2H).

LC-MS:  $t_{\text{R}}$  = 1.85 min, calcd for  $\text{C}_{16}\text{H}_9\text{O}_6^-$  [ $\text{M} - \text{H}$ ] $^-$  297.04  $m/z$ , found 297.11  $m/z$ .

*2,5-Dioxopyrrolidin-1-yl 4-(7,8-Bis(benzyloxy)-4-oxo-4H-chromen-2-yl)benzoate (11)*. In a dry 50 mL flask **10** (198.9 mg, 0.42 mmol), 101.6 mg of EDC·HCl (0.53 mmol, 1.25 equiv), and 64.6 mg of *N*-hydroxysuccinimide (0.56 mmol, 1.33 equiv) in 30 mL of anhydrous THF were heated to 40 °C and stirred overnight. The solvent was removed, and the residue was washed with isopropyl alcohol and ether and dried under vacuum, giving 179.6 mg of the product (75%).

$^1\text{H}$  NMR (400 MHz, DMSO-*d*<sub>6</sub>)  $\delta$  8.25–8.13 (m, 4H), 7.78 (d,  $J$  = 9.0 Hz, 1H), 7.58–7.25 (m, 11H), 7.11 (s, 1H), 5.36 (s, 2H), 5.20 (s, 2H), 2.91 (s, 4H).

*1-Amino-3,6,9,12-tetraoxapentadecan-15-oic Acid (4)*. In a 25 mL flask, 40.3 mg (0.11 mmol) of the *N*-tBoc amide of **4** in 3 mL of DCM was treated with 3 mL of trifluoroacetic acid. After stirring for 2 h, the solvent was removed, and completion of *N*-Boc deprotection was verified by  $^1\text{H}$  NMR.

$^1\text{H}$  NMR (400 MHz, acetone-*d*<sub>6</sub>)  $\delta$  12.27 (s, 1H), 7.49 (s, 1H), 3.92–3.81 (m, 2H), 3.80–3.56 (m, 14H), 3.38 (h,  $J$  = 5.7 Hz, 2H), 2.58 (t,  $J$  = 30.4, 6.1 Hz, 2H).

*1-(4-(7,8-Bis(benzyloxy)-4-oxo-4H-chromen-2-yl)phenyl)-1-oxo-5,8,11,14-tetraoxa-2-azaheptadecan-17-oic Acid (12)*. In a 25 mL flask, the pH of a solution of 29.1 mg of **4** (0.11 mmol) in 1 mL of anhydrous DMF was made basic by a few drops of freshly distilled TEA and treated dropwise with a solution of 61.6 mg (0.107 mmol, 1 equiv) of **11** in 2.5 mL of anhydrous DMF. The resulting mixture was stirred for 6 h at rt. The solvent was removed by evaporation under vacuum, and the residue was dissolved in 10 mL of chloroform. The organic

layer was washed with 30 mL 0.1 M HCl (3×), followed by brine, and then dried over sodium sulfate. Removal of the solvent by evaporation left the product as a solid, 17.2 mg (21.5%), which was used in the next reaction without further purification.

<sup>1</sup>H NMR (400 MHz, CDCl<sub>3</sub>) δ 7.92–7.79 (m, 4H), 7.47–7.21 (m, 11H), 7.06 (d, *J* = 9.0 Hz, 1H), 6.84 (s, 1H), 5.21 (s, 2H), 5.14 (s, 2H), 3.74–3.49 (m, 18H), 2.51 (t, *J* = 5.8 Hz, 2H).

**2,5-Dioxopyrrolidin-1-yl-1-(4-(7,8-bis(benzyloxy)-4-oxo-4H-chromen-2-yl)phenyl)-1-oxo-5,8,11,14-tetraoxa-2-azahaptadecan-17-oate (13).** In a 25 mL flask, 17.2 mg of **12** (0.024 mmol) in 5 mL of THF was treated with 2 equiv of *N*-hydroxysuccinimide (6.25 mg, 0.054 mmol) and with EDC·HCl (14.55 mg, 0.076 mmol). The reaction mixture was stirred overnight. After the solvent was removed by evaporation, the residue was dissolved in 15 mL of chloroform. The organic layer was washed with 30 mL of water, followed by brine, and then dried over sodium sulfate. Evaporation of the solvent left 16.0 mg of **13** (82%), which was used in the next step without further purification.

<sup>1</sup>H NMR (400 MHz, CDCl<sub>3</sub>): δ 7.89–7.78 (m, 5H), 7.44–7.21 (m, 10H), 7.11 (s, 1H), 7.05 (d, *J* = 9.0 Hz, 1H), 6.70 (s, 1H), 5.21 (s, 2H), 5.14 (s, 2H), 3.71 (t, *J* = 6.4 Hz, 2H), 3.66–3.51 (m, 16H), 2.75 (m, 6H).

ESI-MS: calcd for C<sub>45</sub>H<sub>46</sub>N<sub>2</sub>O<sub>13</sub>Na<sup>+</sup> 845.29 *m/z*; found [M + Na]<sup>+</sup> 845.4 *m/z*

**2,5-Dioxopyrrolidin-1-yl-1-(4-(7,8-dihydroxy-4-oxo-4H-chromen-2-yl)phenyl)-1-oxo-5,8,11,14-tetraoxa-2-azahaptadecan-17-oate (14).** In a 25 mL flask, 16.0 mg of **13** (0.019 mmol) in 20 mL of 1:1 v/v THF:ethanol was treated with 30% w/w of Pd catalyst (1:1 w/w Pd/C: Pd(OH)<sub>2</sub>/C, 5.0 mg). The reaction mixture was frozen, pumped out, thawed, and flushed with N<sub>2</sub> (3×) and H<sub>2</sub> (1×) before being stirred overnight under 1 atm of H<sub>2</sub>. The catalyst was filtered off, and the solvent was removed, giving **14** in quantitative yield, which was used in the next step without further purification.

<sup>1</sup>H NMR (400 MHz, CD<sub>3</sub>OD) δ 8.04 (d, *J* = 8.4 Hz, 2H), 7.91 (d, *J* = 8.5 Hz, 2H), 7.54 (d, *J* = 8.7 Hz, 1H), 6.91 (d, *J* = 8.8 Hz, 1H), 6.73 (s, 1H), 3.64–3.53 (m, 18H), 2.84–2.72 (m, 6H).

ESI-MS: calcd for C<sub>31</sub>H<sub>34</sub>N<sub>2</sub>O<sub>13</sub>Na<sup>+</sup> 665.20 *m/z*; found [M + Na]<sup>+</sup> 665.5 *m/z*.

**1-(1-(4-(7,8-Dihydroxy-4-oxo-4H-chromen-2-yl)phenyl)-20-hydroxy-1,17-dioxo-5,8,11,14-tetraoxa-2,18-diazahenicosan-21-yl)-3-(2-hydroxy-2,2-diphosphonoethyl)pyridin-1-ium (5).** **14** (17.0 mg, 0.026 mmol) in 800 μL of THF was added dropwise to 34.4 mg of **15** (0.060 mmol, 2.3 equiv) in 800 μL of water (pH first adjusted to 8.3 with solid sodium carbonate), and the reaction mixture was stirred overnight. The solvent was removed by evaporation, and the residue was dissolved in water. The crude product was purified by reversed-phase (RP) HPLC on a C18 column (21.2 mm × 250 mm, 5 μm, 100 Å pore size), flow rate 8.0 mL/min, using 10% MeCN 0.1 M TEAC (pH 7.0) as buffer A and 75% MeCN 0.1 M TEAC (pH 7.8) as buffer B with the gradient increased to 40% of buffer B over 25 min, followed by elution with 100% of buffer B for 75 min. The desired product was collected (3.0 mg, 13%) and redissolved in a 70% MeOH, 0.1 M ammonium acetate buffer (pH 5.0) (UV, 260 nm).

<sup>1</sup>H NMR (400 MHz, D<sub>2</sub>O): δ 8.82 (s, 1H), 8.60 (dd, *J* = 26.4, 7.0 Hz, 2H), 8.27 (d, *J* = 6.9 Hz, 2H), 8.08 (d, *J* = 7.5 Hz, 2H), 8.01–7.86 (m, 1H), 7.39 (s, 1H), 7.26 (d, *J* = 8.6 Hz,

1H), 6.90 (d, *J* = 8.5 Hz, 1H), 6.61 (s, 1H), 4.41 (dd, *J* = 13.2, 9.7 Hz, 1H), 4.21 (s, 1H), 3.85–3.02 (m, 26H), 2.91 (d, *J* = 22.6 Hz, 4H), 2.73 (s, 3H), 2.46 (t, *J* = 5.9 Hz, 2H).

<sup>31</sup>P NMR (162 MHz, D<sub>2</sub>O) δ 15.6–16.7 (br, 2P).

ESI-MS: calcd for C<sub>37</sub>H<sub>46</sub>N<sub>3</sub>O<sub>18</sub>P<sub>2</sub><sup>-</sup> 882.23 *m/z*; found [M – 2H]<sup>-</sup> 882.4 *m/z*.

**In Vitro Spiral Ganglion Neurite Outgrowth Model.** P4 CBA/CaJ pups were euthanized, and cochleae were dissected from the temporal bone as previously described.<sup>48</sup> The stria vascularis and the sensory epithelium were then removed, exposing the modiolus containing SGN from the modiolus. The SGN population was sharply dissected horizontally and vertically, resulting in 4 pieces.

A 4 well dish plate (CellStar) was prepared by adding sterilized glass coverslips to the wells. Plates were covered with a 1:10 dilution of Matrigel (Corning) for 10 min at 37 °C for SGN outgrowth experiments. Right before plating, plates were washed with HBSS (ThermoFisher Scientific). Each dissected SGN was plated onto the glass plate with the tissue was plated 50 μL of culture medium [DMEM/F12 (GIBCO), N2 (ThermoFisher), B27 (ThermoFisher), 50 μg/mL Ampicillin (Sigma-Aldrich), 1:300 Fungizone (250 μg/mL, GIBCO), and 1:100 Hepes (1 M GIBCO)]. The tissues adhered overnight at 37 °C, 5% CO<sub>2</sub>. All drugs were kept as stock solutions in DMSO at 400 μM and stored at –20 °C. After attachment was confirmed under the microscope, SGNs were treated in darkness with drugs diluted in culture medium at a final concentration of 400 nM. Treatments consisted of Risedronate, 7,8-DHF, Ris-DHF, or DMSO alone (control). Cultures were kept at 37 °C, and drug medium was exchanged every 24 h. After 48 h, the samples were fixed with 4% paraformaldehyde for immunohistochemical analysis. Cultures were permeabilized and blocked with blocking solution (15% goat serum and 0.3% Triton X-100 in PBS), and primary antibodies for neurons mouse TuJ1 (1:500, Biolegend, #801201) were diluted in antibody solution (10% goat serum and 0.1% Triton X-100 in PBS) and applied to cultures overnight at 4 °C. After several washing steps with 1× PBS, fluorescent secondary antibody goat anti-mouse Alexa Fluor 568 (1:500, ThermoFisher, #A-11004) was diluted in antibody medium and incubated for 1 h at rt. Nuclei were stained with DAPI (Thermo Fisher). Tissues were then visualized with Leica SP8 confocal microscopy.

**In Vitro Hydroxyapatite Outgrowth Assays.** HA nanopowder (Sigma-Aldrich) (10 mg) was suspended in 1 mL of culture medium and passed through a 40 μm sterile filter to remove agglutinated nanoparticles. All samples, each containing ~500 μg of nanopowder, were prepared in darkness due to light sensitivity of the compounds. Five 1 mL suspensions of HA with medium containing 8 nM of FAM-Ris (1:50 relative to the other compounds added) as fluorescent label were prepared. Risedronate, Ris-DHF, DMSO alone, and DHF (Abcam) was added to each dilution at a final concentration of 400 nM. After brief vortexing, the samples were incubated at 37 °C.

After 1 h, the particles were centrifuged at 2000 rpm for 2 min, and the supernatant was removed. The residues were washed 4× with fresh medium. HA pellets were then resuspended in 50 μL of 1:5 Matrigel/medium mix (Corning). The Matrigel-HA solution was then spread onto round glass coverslips and placed in the incubator at 37 °C to set for 15 min. SGNs were plated onto the solidified Matrigel-HA suspension for 48 h, and outgrowth was analyzed as described above.

**In Vitro Spiral Ganglion Neurite ANA12 Outgrowth Assay.** SGN samples were dissected and plated as described above. After the tissues had adhered to the plate for 5 h at 37 °C, 5% CO<sub>2</sub>, SGN samples receiving ANA12 had media changed to 50 μL of culture medium containing ANA12 (Tocris Bioscience) at a final concentration of 10 nM. Control samples were incubated overnight without ANA12. ANA12 was stored as stock solution in DMSO at 10 μM at −20 °C. All tissues in both plates were incubated overnight at 37 °C, 5% CO<sub>2</sub>.

After 24 h, all cultures received 400 nM of DHF, Ris, Ris-DHF, or DMSO alone (control) as described above. SGNs in the ANA12 assay plate additionally received 10 nM ANA12 in culture medium. Cultures were kept at 37 °C, and media was changed every 24 h. After 48 h, the cells were fixed, permeabilized, stained, and evaluated with confocal microscopy as described above.

**Neurite Tracing Analysis.** Neurite tracing was performed in blinded fashion. Confocal microscopy z-stack images were analyzed in 3D space with ImageJ and Fiji Software (version 444 K 1.51n NIH public domain). Using the “Analyze-Set Scale” function, the pixel unit of neurite length measurement was set in micrometers. Images were rendered with segmentation function, and Neurite tracer function was applied choosing the starting point at the SGN cell bodies. This allowed for a tracing of the neurite path in 3D through each z-stack in the image file, resulting in a compiled skeleton render of all measured neurites. Only those neurites contained entirely within the image were analyzed. Single neurite lengths and average outgrowth length were then compared between drug treatments.

**In Vitro Cochlear Synaptopathy Model.** For OC explants, P4 CBA/CaJ pups were euthanized, and the cochlea were harvested in similar fashion as described above. The stria vascularis was removed, and the OC was left attached to the modiolus. The middle turn was dissected and separated into 2 pieces using microscissors. The tissue was plated on Laminin (20 μg/mL, 37 °C overnight, ThermoFisher) and poly-L-ornithine 0.01% (Millipore, 2 h at 37 °C) pretreated 4-well culture dishes with glass coverslips. Explants attached overnight in culture medium as described above. After attachment was confirmed microscopically, explants were treated in darkness with 0.5 mM KA (Abcam) diluted in culture medium for 2 h. An untreated explant was kept as negative control, and a second explant treated with KA only was kept as positive control. KA medium was removed, and after washing with prewarmed medium, explants were treated in darkness with Ris 400 nM, DHF 400 nM, or Ris-DHF 400 nM diluted in medium. After 24 h of exposure to drug, explants were fixed and permeabilized as described above. Presynaptic ribbon synapses were stained with CtBP2 (IgG1, mouse, 1:200, #612044, BD Biosciences), while the postsynaptic neural synapse portion was labeled with PSD95 (IgG2a, mouse, 1:50, #75-028, Neuromab). Nerve fibers were stained with Neurofilament (NF-H, chicken, 1:2500, #AB5539, Millipore), and hair cells were labeled with Myosin VIIa (Myo7a, rabbit, #25-6790, Proteus). Alexa Fluor antibodies (Invitrogen, 1:500) were used for fluorescent secondary labeling (goat anti-mouse IgG1 488, goat anti-mouse IgG2a 568, goat anti-rabbit 647, goat anti-chicken 647). Explants were imaged with a Leica SP8 confocal microscope, visualizing the entire hair cell with the synaptic pole, at a z-step-size of 0.25 μm.

**Synaptic Ribbon Quantification and Colocalization Analysis.** Colocalization image analysis was performed by an observer blinded to sample identity. Image stacks were imported to Amira v6.0. Isosurface Rendering and Image Orthoprojections functions were used to create 3D renderings of the image stacks for counting as previously described.<sup>5,6,49</sup>

## CONCLUSIONS

A rationally designed conjugate of 7,8-DHF (1), a TrkB agonist, linked to a bone mineral-targeting bisphosphonate, Ris-DHF (5), was synthesized in nine steps and found to retain the ability of DHF to support SGN neurite outgrowth between cochlear hair cells and spiral ganglion neurons. Strikingly, the ability of Ris-DHF to promote spiral ganglion neurite outgrowth is enhanced following adsorption to hydroxyapatite, which mimics bone mineral. Finally, we have shown that Ris-DHF promotes regeneration of ribbon synapses between hair cells and spiral ganglion neurons using an *in vitro* excitotoxic assay. Taken together, these findings provide strong preliminary evidence that cochlea-targeted delivery of a neurotrophic agonist linked to a BP is a promising strategy to regenerate ribbon synapses following noise damage or aging in the mammalian cochlea.

## ASSOCIATED CONTENT

### Supporting Information

The Supporting Information is available free of charge on the ACS Publications website at DOI: 10.1021/acs.bioconjchem.8b00022.

Chromatography traces and NMR and MS spectra with experimental details for the preliminary synthetic studies (PDF).

## AUTHOR INFORMATION

### Corresponding Authors

\*E-mail: david\_jung@meei.harvard.edu

\*E-mail: mckenna@usc.edu

### ORCID

Charles E. McKenna: 0000-0002-3540-6663

### Author Contributions

J.S.K., K.N., and C.H. contributed equally. C.E.M. and D.H.J. conceived the project and wrote the manuscript. C.E.M. and B.A.K. designed the synthetic work, which was carried out by K.N. D.H.J. and A.S.E. designed the biological studies, which were carried out by C.H., J.S.K., and N.K. All authors have given approval to the final version of the manuscript.

### Notes

The authors declare no competing financial interest.

## ACKNOWLEDGMENTS

We thank Ms. Inah Kang for her invaluable assistance in the preparation of this manuscript and Prof. M. Charles Liberman for initial guidance in 3-D imaging of synapses. This work was supported by the American Academy of Otolaryngology-Head and Neck Surgery Herbert Silverstein Otology and Neurotology Research Award, the American Otological Society Research Grant, and by a grant from the National Institute of Deafness and other Communicative Disorders, R01 DC007174.

## ■ ABBREVIATIONS

SNHL, sensorineural hearing loss; SGN, spiral ganglion neuron; DHF, 7,8-dihydroxyflavone; TrkB, tropomyosin receptor kinase B; BP, bisphosphonate; RWM, round window membrane; KA, kainic acid; OC, organ of Corti; Ris, risedronate; Zol, zoledronate; Ris-DHF, risedronate-DHF conjugate; HA, hydroxyapatite

## ■ REFERENCES

- (1) Lin, F. R., Thorpe, R., Gordon-Salant, S., and Ferrucci, L. (2011) Hearing loss prevalence and risk factors among older adults in the United States. *J. Gerontol., Ser. A* 66A, 582–590.
- (2) Schuknecht, H. F., and Gacek, M. R. (1993) Cochlear pathology in presbycusis. *Ann. Otol., Rhinol., Laryngol.* 102, 1–16.
- (3) Sergeyenko, Y., Lall, K., Liberman, M. C., and Kujawa, S. G. (2013) Age-related cochlear synaptopathy: an early-onset contributor to auditory functional decline. *J. Neurosci.* 33, 13686–13694.
- (4) Viana, L. M., O'Malley, J. T., Burgess, B. J., Jones, D. D., Oliveira, C. A., Santos, F., Merchant, S. N., Liberman, L. D., and Liberman, M. C. (2015) Cochlear neuropathy in human presbycusis: Confocal analysis of hidden hearing loss in post-mortem tissue. *Hear. Res.* 327, 78–88.
- (5) Kujawa, S. G., and Liberman, M. C. (2006) Acceleration of age-related hearing loss by early noise exposure: evidence of a misspent youth. *J. Neurosci.* 26, 2115–2123.
- (6) Kujawa, S. G., and Liberman, M. C. (2009) Adding insult to injury: cochlear nerve degeneration after "temporary" noise-induced hearing loss. *J. Neurosci.* 29, 14077–14085.
- (7) Bharadwaj, H. M., Verhulst, S., Shaheen, L., Liberman, M. C., and Shinn-Cunningham, B. G. (2014) Cochlear neuropathy and the coding of supra-threshold sound. *Front. Syst. Neurosci.* 8, 26.
- (8) Stankovic, K., Rio, C., Xia, A., Sugawara, M., Adams, J. C., Liberman, M. C., and Corfas, G. (2004) Survival of adult spiral ganglion neurons requires erbB receptor signaling in the inner ear. *J. Neurosci.* 24, 8651–8661.
- (9) Nadol, J. B., Jr. (1997) Patterns of neural degeneration in the human cochlea and auditory nerve: implications for cochlear implantation. *Otolaryngol. Head Neck Surg.* 117, 220–228.
- (10) Muller, U., and Barr-Gillespie, P. G. (2015) New treatment options for hearing loss. *Nat. Rev. Drug Discovery* 14, 346–365.
- (11) Ernfors, P., Kucera, J., Lee, K. F., Loring, J., and Jaenisch, R. (1995) Studies on the physiological role of brain-derived neurotrophic factor and neurotrophin-3 in knockout mice. *Int. J. Dev. Biol.* 39, 799–807.
- (12) Terenghi, G. (1999) Peripheral nerve regeneration and neurotrophic factors. *J. Anat.* 194 (Pt 1), 1–14.
- (13) Evans, A. J., Thompson, B. C., Wallace, G. G., Millard, R., O'Leary, S. J., Clark, G. M., Shepherd, R. K., and Richardson, R. T. (2009) Promoting neurite outgrowth from spiral ganglion neuron explants using polypyrrole/BDNF-coated electrodes. *J. Biomed. Mater. Res., Part A* 91A, 241–250.
- (14) Takada, Y., Beyer, L. A., Swiderski, D. L., O'Neal, A. L., Prieskorn, D. M., Shivatzi, S., Avraham, K. B., and Raphael, Y. (2014) Connexin 26 null mice exhibit spiral ganglion degeneration that can be blocked by BDNF gene therapy. *Hear. Res.* 309, 124–135.
- (15) Shibata, S. B., Cortez, S. R., Beyer, L. A., Wiler, J. A., Di Polo, A., Pflugst, B. E., and Raphael, Y. (2010) Transgenic BDNF induces nerve fiber regrowth into the auditory epithelium in deaf cochleae. *Exp. Neurol.* 223, 464–472.
- (16) Wan, G., Gomez-Casati, M. E., Gigliello, A. R., Liberman, M. C., and Corfas, G. (2014) Neurotrophin-3 regulates ribbon synapse density in the cochlea and induces synapse regeneration after acoustic trauma. *eLife* 3, e03564.
- (17) Suzuki, J., Corfas, G., and Liberman, M. C. (2016) Round-window delivery of neurotrophin 3 regenerates cochlear synapses after acoustic overexposure. *Sci. Rep.* 6, 24907.
- (18) Swan, E. E., Mescher, M. J., Sewell, W. F., Tao, S. L., and Borenstein, J. T. (2008) Inner ear drug delivery for auditory applications. *Adv. Drug Delivery Rev.* 60, 1583–1599.
- (19) Budenz, C. L., Wong, H. T., Swiderski, D. L., Shibata, S. B., Pflugst, B. E., and Raphael, Y. (2015) Differential effects of AAV.BDNF and AAV.Ntf3 in the deafened adult guinea pig ear. *Sci. Rep.* 5, 8619.
- (20) Sly, D. J., Campbell, L., Uschakov, A., Saief, S. T., Lam, M., and O'Leary, S. J. (2016) Applying Neurotrophins to the Round Window Rescues Auditory Function and Reduces Inner Hair Cell Synaptopathy After Noise-induced Hearing Loss. *Otol. Neurotol.* 37, 1223–1230.
- (21) Ramekers, D., Versnel, H., Strahl, S. B., Klis, S. F., and Grolman, W. (2015) Temporary Neurotrophin Treatment Prevents Deafness-Induced Auditory Nerve Degeneration and Preserves Function. *J. Neurosci.* 35, 12331–12345.
- (22) Ramekers, D., Versnel, H., Grolman, W., and Klis, S. F. (2012) Neurotrophins and their role in the cochlea. *Hear. Res.* 288, 19–33.
- (23) Goycoolea, M. V. (2001) Clinical aspects of round window membrane permeability under normal and pathological conditions. *Acta Otolaryngol.* 121, 437–447.
- (24) Jang, S. W., Liu, X., Yepes, M., Shepherd, K. R., Miller, G. W., Liu, Y., Wilson, W. D., Xiao, G., Blanchi, B., Sun, Y. E., et al. (2010) A selective TrkB agonist with potent neurotrophic activities by 7,8-dihydroxyflavone. *Proc. Natl. Acad. Sci. U. S. A.* 107, 2687–2692.
- (25) Yu, Q., Chang, Q., Liu, X., Wang, Y., Li, H., Gong, S., Ye, K., and Lin, X. (2013) Protection of spiral ganglion neurons from degeneration using small-molecule TrkB receptor agonists. *J. Neurosci.* 33, 13042–13052.
- (26) Tong, M., Fernandez, K. A., Lall, K., Kujawa, S. G., and Edge, A. (2014) In *Annual Meeting of the Association for Research in Otolaryngology*, San Diego.
- (27) Plontke, S. K., Glien, A., Rahne, T., Mader, K., and Salt, A. N. (2014) Controlled release dexamethasone implants in the round window niche for salvage treatment of idiopathic sudden sensorineural hearing loss. *Otol. Neurotol.* 35, 1168–1171.
- (28) Salt, A. N., and Plontke, S. K. (2009) Principles of local drug delivery to the inner ear. *Audiol. Neuro-Otol.* 14, 350–360.
- (29) Ebetino, F. H., Hogan, A. M., Sun, S., Tsoumpra, M. K., Duan, X., Triffitt, J. T., Kwaasi, A. A., Dunford, J. E., Barnett, B. L., Oppermann, U., et al. (2011) The relationship between the chemistry and biological activity of the bisphosphonates. *Bone* 49, 20–33.
- (30) Kashemirov, B. A., Bala, J. L., Chen, X., Ebetino, F. H., Xia, Z., Russell, R. G. G., Coxon, F. P., Roelofs, A. J., Rogers, M. J., and McKenna, C. E. (2008) Fluorescently Labeled Risedronate and Related Analogues: "Magic Linker" Synthesis. *Bioconjugate Chem.* 19 (12), 2308–2310.
- (31) Roelofs, A. J., Stewart, C. A., Sun, S., Blazewska, K. M., Kashemirov, B. A., McKenna, C. E., Russell, R. G., Rogers, M. J., Lundy, M. W., Ebetino, F. H., et al. (2012) Influence of bone affinity on the skeletal distribution of fluorescently labeled bisphosphonates in vivo. *J. Bone Miner. Res.* 27, 835–847.
- (32) Sedghizadeh, P. P., Sun, S., Junka, A. F., Richard, E., Sadrafi, K., Mahabady, S., Bakhshalian, N., Tjokro, N., Bartoszewicz, M., Oleksy, M., et al. (2017) Design, Synthesis, and Antimicrobial Evaluation of a Novel Bone-Targeting Bisphosphonate-Ciprofloxacin Conjugate for the Treatment of Osteomyelitis Biofilms. *J. Med. Chem.* 60, 2326–2343.
- (33) Roelofs, A. J., Coxon, F. P., Ebetino, F. H., Lundy, M. W., Henneman, Z. J., Nancollas, G. H., Sun, S., Blazewska, K. M., Bala, J. L., Kashemirov, B. A., et al. (2010) Fluorescent risedronate analogues reveal bisphosphonate uptake by bone marrow monocytes and localization around osteocytes in vivo. *J. Bone Miner. Res.* 25, 606–616.
- (34) Sun, S., Blazewska, K. M., Kadina, A. P., Kashemirov, B. A., Duan, X., Triffitt, J. T., Dunford, J. E., Russell, R. G., Ebetino, F. H., Roelofs, A. J., et al. (2016) Fluorescent Bisphosphonate and Carboxyphosphonate Probes: A Versatile Imaging Toolkit for Applications in Bone Biology and Biomedicine. *Bioconjug. Chem.* 27, 329–340.

(35) Kang, W. S., Sun, S., Nguyen, K., Kashemirov, B., McKenna, C. E., Hacking, S. A., Quesnel, A. M., Sewell, W. F., McKenna, M. J., and Jung, D. H. (2015) Non-Ototoxic Local Delivery of Bisphosphonate to the Mammalian Cochlea. *Otol. Neurotol.* 36, 953–960.

(36) Quesnel, A. M., Seton, M., Merchant, S. N., Halpin, C., and McKenna, M. J. (2012) Third-generation bisphosphonates for treatment of sensorineural hearing loss in otosclerosis. *Otol. Neurotol.* 33, 1308–1314.

(37) Bertrand, T., Kothe, M., Liu, J., Dupuy, A., Rak, A., Berne, P. F., Davis, S., Gladysheva, T., Valtre, C., Crenne, J. Y., et al. (2012) The crystal structures of TrkA and TrkB suggest key regions for achieving selective inhibition. *J. Mol. Biol.* 423, 439–453.

(38) Trott, O., and Olson, A. J. (2010) AutoDock Vina: improving the speed and accuracy of docking with a new scoring function, efficient optimization, and multithreading. *J. Comput. Chem.* 31, 455–461.

(39) Nguyen, K., Kang, W. S., Jung, D. H., Sewell, W. F., Kashemirov, B. A., McKenna, C. E., and McKenna, M. J. (2016) In *2016 World Molecular Imaging Congress*, New York, NY.

(40) Sun, H., Chen, F., Wang, X., Liu, Z., Yang, Q., Zhang, X., Zhu, J., Qiang, L., Guo, Q., and You, Q. (2012) Studies on gambogic acid (IV): Exploring structure-activity relationship with IkappaB kinase-beta (IKKbeta). *Eur. J. Med. Chem.* 51, 110–123.

(41) Soppet, D., Escandon, E., Maragos, J., Middlemas, D. S., Reid, S. W., Blair, J., Burton, L. E., Stanton, B. R., Kaplan, D. R., Hunter, T., et al. (1991) The neurotrophic factors brain-derived neurotrophic factor and neurotrophin-3 are ligands for the trkB tyrosine kinase receptor. *Cell* 65, 895–903.

(42) Klein, R., Nanduri, V., Jing, S. A., Lamballe, F., Tapley, P., Bryant, S., Cordon-Cardo, C., Jones, K. R., Reichardt, L. F., and Barbacid, M. (1991) The trkB tyrosine protein kinase is a receptor for brain-derived neurotrophic factor and neurotrophin-3. *Cell* 66, 395–403.

(43) Liu, X., Obianyo, O., Chan, C. B., Huang, J., Xue, S., Yang, J. J., Zeng, F., Goodman, M., and Ye, K. (2014) Biochemical and biophysical investigation of the brain-derived neurotrophic factor mimetic 7,8-dihydroxyflavone in the binding and activation of the TrkB receptor. *J. Biol. Chem.* 289, 27571–27584.

(44) Cazorla, M., Premont, J., Mann, A., Girard, N., Kellendonk, C., and Rognan, D. (2011) Identification of a low-molecular weight TrkB antagonist with anxiolytic and antidepressant activity in mice. *J. Clin. Invest.* 121, 1846–1857.

(45) Wang, Q., and Green, S. H. (2011) Functional role of neurotrophin-3 in synapse regeneration by spiral ganglion neurons on inner hair cells after excitotoxic trauma in vitro. *J. Neurosci.* 31, 7938–7949.

(46) Nguyen, K., Kempfle, J. S., Jung, D. H., and McKenna, C. E. (2017) Recent advances in therapeutics and drug delivery for the treatment of inner ear diseases: a patent review (2011–2015). *Expert Opin. Ther. Pat.* 27, 191–202.

(47) Kao, S. Y., Kempfle, J. S., Jensen, J. B., Perez-Fernandez, D., Lysaght, A. C., Edge, A. S., and Stankovic, K. M. (2013) Loss of osteoprotegerin expression in the inner ear causes degeneration of the cochlear nerve and sensorineural hearing loss. *Neurobiol. Dis.* 56, 25–33.

(48) Parker, M., Brugeaud, A., and Edge, A. S. (2010) Primary culture and plasmid electroporation of the murine organ of Corti. *J. Vis. Exp.* 36, 1685.

(49) Kujawa, S. G., and Liberman, M. C. (2015) Synaptopathy in the noise-exposed and aging cochlea: Primary neural degeneration in acquired sensorineural hearing loss. *Hear. Res.* 330, 191–199.